MaxQuant.Live Enables Global Targeting of More Than 25,000 Peptides

Authors

Christoph Wichmann, Florian Meier, Sebastian Virreira Winter, Andreas-David Brunner, Jürgen Cox, and Matthias Mann

Correspondence

mmann@biochem.mpg.de;
cox@biochem.mpg.de

In Brief

MaxQuant.Live builds on the fast application programming interface of quadrupole Orbitrap mass analyzers to control data acquisition in real-time (freely available at www.maxquant.live). Its graphical user interface enables advanced data acquisition strategies, such as in-depth characterization of peptides of interest. Online recalibration in mass, retention time, and intensity dimensions extends this concept to more than 25,000 peptides per run. Our "global targeting" strategy combines the best of targeted and shotgun approaches.

Graphical Abstract
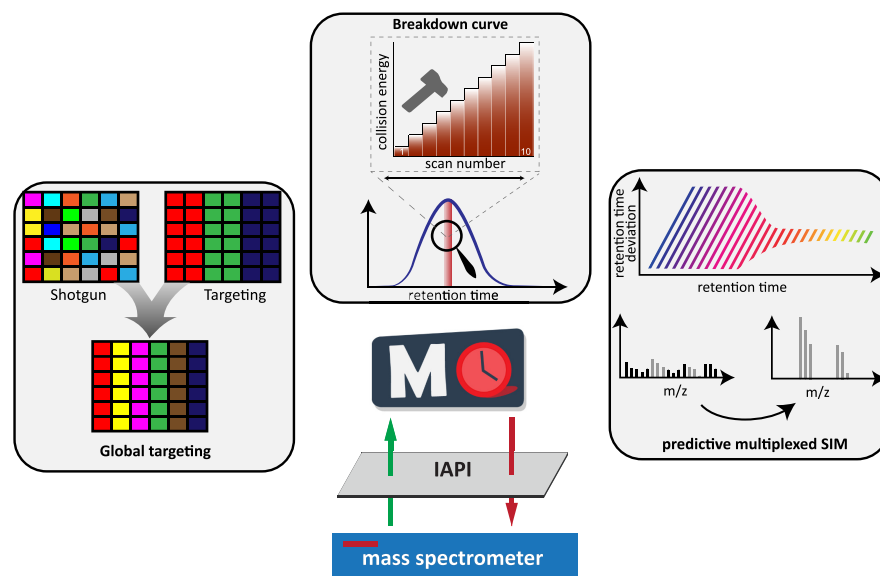
Highlights

- MaxQuant.Live controls Orbitrap mass analyzers in real-time.

- Freely available apps enable advanced data acquisition strategies.

- On-the-fly mass, retention time and intensity recalibration.

- Global targeting unifies shotgun and targeted proteomics.

⌘ *Author's Choice*

MaxQuant.Live Enables Global Targeting of More Than 25,000 Peptides

Ⓘ**Christoph Wichmann‡,** Ⓘ**Florian Meier§¶,** Ⓘ**Sebastian Virreira Winter§,**
Ⓘ**Andreas-David Brunner§,** Ⓘ**Jürgen Cox‡**, and** Ⓘ**Matthias Mann§¶‖**

Mass spectrometry (MS)-based proteomics is often performed in a shotgun format, in which as many peptide precursors as possible are selected from full or MS1 scans so that their fragment spectra can be recorded in MS2 scans. Although achieving great proteome depths, shotgun proteomics cannot guarantee that each precursor will be fragmented in each run. In contrast, targeted proteomics aims to reproducibly and sensitively record a restricted number of precursor/fragment combinations in each run, based on prescheduled mass-to-charge and retention time windows. Here we set out to unify these two concepts by a global targeting approach in which an arbitrary number of precursors of interest are detected in real-time, followed by standard fragmentation or advanced peptide-specific analyses. We made use of a fast application programming interface to a quadrupole Orbitrap instrument and real-time recalibration in mass, retention time and intensity dimensions to predict precursor identity. MaxQuant.Live is freely available (www.maxquant.live) and has a graphical user interface to specify many predefined data acquisition strategies. Acquisition speed is as fast as with the vendor software and the power of our approach is demonstrated with the acquisition of breakdown curves for hundreds of precursors of interest. We also uncover precursors that are not even visible in MS1 scans, using elution time prediction based on the auto-adjusted retention time alone. Finally, we successfully recognized and targeted more than 25,000 peptides in single LC-MS runs. Global targeting combines the advantages of two classical approaches in MS-based proteomics, whereas greatly expanding the analytical toolbox. *Molecular & Cellular Proteomics 18: 982–994, 2019. DOI: 10.1074/mcp.TIR118.001131.*

Mass spectrometry (MS)-based proteomics has matured into a versatile and widely used analytical tool in the life sciences (1–3). State-of-the-art workflows cover the proteome of model organisms to near-completeness and sensitivity extends into the attomole range (4–7). Still, many, and in particular low-abundance, proteins escape accurate and reproducible quantification across large sets of biological samples, which hinders wider applications of proteomics in systems biology and translational medicine (8, 9). In part, this is because of the complexity of bottom-up proteomics samples. Enzymatic digestions of protein extracts are comprised of millions of peptide species and, even with liquid chromatography, many peptides co-elute, spanning several orders of magnitude in abundance (10). In data-dependent acquisition schemes (DDA)[1], the mass spectrometer acquires as many MS2 spectra as possible to maximize the number of peptide identifications. As high-abundance ions are more likely to yield high-quality MS2 spectra, precursors are typically prioritized for isolation and fragmentation by their abundance and dynamic exclusion is employed to prevent their resequencing. This topN approach has been the method of choice for unbiased and comprehensive proteomic studies for many years. However, given the enormous number of precursor candidates and unavoidable run-to-run variabilities, a specific peptide may not be fragmented in every run. Data-independent acquisition (DIA) aims to avoid stochasticity by repeatedly cycling through fixed isolation windows (11), however, it increases spectral complexity and may diminish dynamic range and by its nature does not address all application scenarios .

In contrast to DDA and DIA, the goals of targeted proteomics methods are to analyze a limited number of selected proteins of interest with maximum sensitivity and reproducibility (12). Rather than selecting precursors based on the MS1 scans, the instrument is instructed to continuously fragment certain predefined precursor-fragment mass combinations during scheduled time windows, in which the targeted peptides are expected.

Traditionally, these experiments have been performed on triple quadrupole instruments, even before the advent of proteomics (13, 14). However, today high-resolution time-of-flight or Orbitrap mass analyzers are gaining popularity. Instead of recording one or a few specified precursor-fragment

transition, these instruments acquire complete MS2 spectra and therefore monitor all fragment ions simultaneously, which increases specificity and quantitative accuracy (15, 16). In practice, setting up a robust targeted proteomics experiment with a desired coverage remains challenging as the number of targets needs to be balanced with acquisition speed and sensitivity (17, 18). Selecting too many targets may unduly reduce the acquisition time for each of them, whereas specifying narrow LC elution windows increases the risk of missing a peptide entirely as the retention times cannot be estimated very accurately beforehand. Reports in the literature generally employ minute-wide monitoring windows to target tens and sometimes hundreds peptides and proteins. Further, despite the creation of community-wide MRM peptide libraries (19–21), these assays are typically reestablished and optimized in each laboratory.

To address some of the above limitations, Domon and co-workers spiked-in isotope-labeled variants of the peptides of interest to trigger "pretargeting" and targeting events more precisely (22). Coon and colleagues used the expected elution order of peptides to bias DDA toward peptides of interest (23). Building on the MaxQuant software suite (24, 25) our own group developed the MaxQuant-RealTime framework, which identified peptides within milliseconds, providing a basis to implement intelligent data acquisition methods in different research scenarios (26). Although these concepts and potential applications are very promising in principle, the uptake of the underlying software packages was limited.

Proteomics post-processing algorithms generally contain a mass recalibration step as well as retention time alignment, which can be used to transfer identifications between runs (24, 27, 28). For instance, MaxQuant can achieve sub-parts-per-million (ppm) mass accuracies and absolute retention time deviations below 30s by nonlinear recalibration and alignment. We reasoned that approaching such an accuracy in real-time could dramatically improve our ability to predict the appearance of a very large number of peptides. This would drastically reduce the monitoring time for each peptide and might allow extending the targeting concept to a global, proteome-wide scale.

To realize this vision, we developed the freely available software MaxQuant.Live, which interacts with any Thermo Fisher Q Exactive mass spectrometer via the redesigned instrument application programing interface (IAPI) (29). Scan modules ("apps") can be plugged into the MaxQuant.Live core application on the acquisition computer, allowing straightforward implementation and modification of standard acquisition schemes as well as advanced data acquisition strategies based on live data analysis.

---

[1] The abbreviations used are: DDA, data-dependent acquisition; GUI, graphical user interface; IAPI, instrument application programing interface; NCE, normalized collision energy; SIM, selected ion monitoring; pmSIM, predictive multiplexed selective ion monitoring.

EXPERIMENTAL PROCEDURES

Cell Culture and Sample Preparation—We cultured the human HeLa cancer cell line (HeLa S3, ATCC, Manassas, VA) in Dulbecco's modified Eagle's medium (DMEM) with 10% fetal bovine serum, 20 mM glutamine and 1% penicillin-streptomycin added (all Life Technologies Ltd., Paisley, UK). Metabolic stable isotope labeling (30) was performed in arginine- and lysine-free DMEM, fortified with arginine and lysine with natural isotope abundances (light channel) or stable-isotope labeled arginine-10 and lysine-8 (Cambridge Isotope Laboratories, Tewksbury, MA) as previously described (31). Cells were collected by centrifugation, washed twice with cold phosphate-buffered saline, pelleted and stored at −80 °C.

We lysed the cells and reduced and alkylated the proteins in a single reaction vial with sodium deoxycholate (SDC) buffer containing chloroacetamide (PreOmics GmbH, Martinsried, Germany) following our previously published protocol (32). Cells were suspended in the SDC buffer and boiled for 10 min at 95 °C. To disrupt remaining cellular structures and shear nucleic acids, we sonicated the suspension for 15 min at full power (Bioruptor, Diagenode, Seraing, Belgium). The crude protein extracts were enzymatically digested with LysC and trypsin (1:100, enzyme wt/protein wt) overnight at 37 °C before stopping the reaction with 5 volumes of isopropanol/1% trifluoroacetic acid (TFA). Peptide micro-purification and de-salting was performed on styrenedivinylbenzene-reversed phase sulfonate StageTips. Following sequential washing steps with isopropanol/1% TFA and water with 0.1% TFA, peptides were eluted with 80% acetonitrile (ACN) containing 1% ammonia. The vacuum dried eluates were reconstituted in water with 2% ACN and 0.1% TFA for further analysis.

Liquid Chromatography and Mass Spectrometry (LC-MS)—In single LC-MS runs, ∼500 ng of purified whole-cell digests were analyzed with an EASY-nLC 1200 nanoflow chromatography system (Thermo Fisher Scientific, Bremen, Germany) coupled online to a hybrid quadrupole Orbitrap mass spectrometer (Thermo Q Exactive HF-X (33)). The peptides were separated at 60 °C on a 50 cm long column (75 μm inner diameter) packed with 1.9 μm porous silica beads (Dr. Maisch, Ammerbuch-Entringen, Germany), and electrosprayed from a laser-pulled silica emitter tip at 2.4 kV. Mobile phases A and B were water with 0.1% formic acid (v/v) and 80/20/0.1% ACN/water/formic acid (v/v/v). To elute the peptides at a constant flow rate of 300 nL/min, a binary gradient was ramped from 5% to 30% B within 95 min, followed by an increase to 60% B within 5 min and further to 95% B for washing. After 5 min, the organic content was decreased to the starting value within 5 min and the column was reequilibrated for another 5 min.

Standard top15 DDA methods were generated with the graphical Thermo Xcalibur method editor. Full MS scans in the mass range from m/z 300 to 1650 were acquired with a 128 ms transient time corresponding to a resolution of 60,000 at m/z 200. The target value for the automatic gain control (AGC) algorithm was set to 3×10^6 charges, which was typically reached within about 1 ms during the elution of peptides. Precursor ions for MS2 scans were isolated with a ±0.7 Th window centered on the precursor mass and fragmented with higher energy collisional dissociation (HCD) (34) at a normalized collision energy (NCE) of 27. MS2 spectra were acquired with a resolution of 15,000 at m/z 200, and the maximum ion injection time and the AGC target were set to 25 ms and 1×10^5 charges, respectively. Only precursors with assigned charge states $> = 2$ and $< = 5$ were considered, and previously sequenced precursors were dynamically excluded for 30 s.

Acquisition Software—MaxQuant.Live (Version 0.1) was continuously running in its "listening mode" on the acquisition computer waiting for a signal to load and execute a scan protocol from the library. To schedule batches of LC-MS runs, we used the sequence list from Xcalibur whose entries contain settings for the LC device as

well as the method for the mass spectrometer. While using the normal LC-settings we constructed the instrument method in such a way that it encodes the start signal for MaxQuant.Live to load a given scan protocol and take over the control of the mass spectrometer for the whole run on starting.

Scan protocols for the different targeting strategies were all specified using the targeting app that is included in MaxQuant.Live. As initial settings for peptide recognition, we chose by default a mass tolerance of ± 10 ppm, a retention time tolerance of ± 3 min and an intensity threshold value of 10^{-5} from the expected intensity of the target. To calculate the corrections, the adaptive correction includes the peptides recognized within the last 3 min but retains a minimum of the last 100. The correction automatically started 6 min after the first peptide was recognized and the mass tolerances were set to 4.5 ppm.

Breakdown Curves—As an example of advanced acquisition schemes enabled by MaxQuant.Live, we studied the large-scale and automated acquisition of HCD fragmentation characteristics of peptides. In triplicate runs of a HeLa digest, we targeted 1000 precursors, using 10,000 endogenous peptides for real-time corrections. On recognition in real-time, precursors were isolated with a ± 0.2 Th window and repeatedly fragmented with increasing collision energy in ten steps from NCE 18 to 36. Other than that, the MS parameters were set as above. Target peptides were selected randomly from the top 50% abundance quantile of peptides identified in a standard DDA run of the same digest after removal of contaminants and reverse hits and filtering for the most abundant evidence of each unique peptide sequence. The tolerances for the real-time correction were the default values listed before.

Predictive Multiplexed Selective Ion Monitoring (pmSIM)—Light and heavy labeled tryptic Hela lysates were mixed in a ratio of 4:1 and 500 ng were injected on column. DDA raw files were analyzed using MaxQuant to identify light to heavy SILAC peptide ratios. To generate a targeting list for MaxQuant.Live, the "evidence" output file was filtered for modified sequence duplicates, missed cleavages, keeping only unmodified peptides with a sequence length less than 25 amino acids, a retention length less than 2 min, no modifications and a charge state of 2. Peptides for retention correction were additionally filtered for >10 and < 80 min retention time, after which the top 5,000 most intense light channel peptides were selected. The fifty peptides for selected ion monitoring (SIM) were randomly chosen from a list fulfilling the following criteria: retention time 20–70 min, no reported L/H ratio, an intensity of zero in the heavy channel. The initial retention time tolerance was ± 10 min and the final value was 1.5-fold of the elution time standard deviation.

MaxQuant.Live pmSIM experiments were performed with a 1 Th isolation window and a $+0.2$ Th offset and acquired with a resolution of 120,000 at *m/z* 200. The heavy and light channels were multiplexed in a single scan. A maximum of 1×10^5 ions were collected in each channel with a maximum ion injection time of 48 and 192 ms for the light and heavy channel, respectively.

Data analysis of the pmSIM experiment was performed with the Skyline (35) (Version 4.1.0.18169) and XCalibur (3.1.66.10) software suites. The SIM targeting raw file was split into SIM and MS1 scans and analyzed independently.

Large-scale Targeting—To build a reference DDA dataset, 500 ng of tryptic Hela digest were measured in triplicate and raw files were analyzed with MaxQuant. The matching between runs feature was activated using the default settings. Peptide identities as well as their mass, charge state, retention time and intensity were extracted from the evidence output file and used to generate targeting lists for MaxQuant.Live. Only peptides with a retention time between 10 and 100 min that were identified by MS/MS or matching in all three replicates were candidates for the targeting lists and any hits from the

reverse decoy library and potential contaminants were excluded from the selection. To generate the targeting lists, 100, 1000, 5000, 10,000, 20,000 or 30,000 peptides were randomly selected from all peptides fulfilling the above criteria, ensuring a uniform distribution of targets over the whole abundance range. For real time correction, we selected the 10,000 most abundant peptides identified by MS/MS or matching in all three replicates with a retention length less than 30 s. The tolerances for real-time correction were the default values listed above. To demonstrate the functionality of the real-time correction we performed an additional run with 20,000 targeting peptides, in which the minimal mass tolerance was 4.5 ppm and the retention time windows size was 2.5-fold of the standard deviation of the peptide elution times. Here, the correction was calculated from all the peptides that were recognized within the last minute but at least the last 20.

Full MS scans in the mass range from *m/z* 300 to 1650 were acquired with a resolution of 60,000 at *m/z* 200 and an automatic gain control (AGC) target of 3×10^6. Target peptides had a "Life Time" (max. time between recognition and fragmentation) of 1000 ms and were isolated for MS2 scans with a $+- 0.2$ Th window centered on the precursor mass and fragmented with a NCE of 27. MS2 spectra were acquired with a resolution of 15,000 at *m/z* 200, and the maximum ion injection time and the AGC target were 110 ms and 1×10^5 charges, respectively. Raw files of the targeting runs were analyzed in MaxQuant together with the standard DDA runs using the matching between runs feature. Coefficients of variation (CVs) were calculated for the targeted peptides between replicate measurements of standard DDA and targeting runs. To normalize for variations in total sample between injections, intensities were median normalized before calculation of CVs.

Proteomics Data Processing—Shotgun proteomics raw data acquired with either the standard user interface or MaxQuant.Live were processed with MaxQuant (24) (version 1.6.1.13) using the default settings if not stated otherwise. The built-in Andromeda search engine (25) scored MS2 spectra against fragment masses of tryptic peptides derived from a human reference proteome containing 95,057 entries including isoforms (UniProt, release 2018/06) and a list of 245 potential contaminants. We required a minimum peptide length of 7 amino acids and limited the search space to a maximum peptide mass of 4600 Da and two missed cleavage sites. Carbamidomethylation of cysteine was specified as a fixed modification, and methionine oxidation and acetylation at protein N termini as variable modifications. MaxQuant uses individual mass tolerances for each peptide, whereas the initial maximum precursor mass tolerances were set to 20 ppm in the first search and 4.5 ppm in the main search, and the fragment mass tolerance was set to 20 ppm. The false discovery rate was controlled with a target-decoy approach at less than 1% for peptide spectrum matches and less than 1% for protein group identifications.

Bioinformatics—Post-processing was performed in either Perseus (36), the R computational environment (37) or the Python programming language. Potential contaminants, reverse database hits and proteins identified by only one modified peptide were excluded from the analysis.

Experimental Design and Statistical Rationale—In this study, we developed the MaxQuant.Live software for MS data acquisition, which enables classical acquisition schemes as well as methods that are more elaborate. We evaluated the technical feasibility of large-scale peptide recognition. Sample sizes were chosen to allow assessing technical variations with replicate LC-MS injections of aliquots from the same sample preparation batch. The n numbers were 1, 1, 3, 3, 3 for the experiments in Figs. 2, 3, 4, 5, and 6, respectively. Statistical testing, control samples and blinding were not applicable, and no data points were excluded. No targeting experiments em-

FIG. 1. **Architecture of Max-Quant.Live and the logic of its scan protocols.** The core of our software (yellow box) handles the real-time control of the mass spectrometer using the IAPI by Thermo Fisher. Its engine processes the scan data according to a scan protocol, which specifies a data-acquisition strategy trough a decision tree logic (right). Scan protocols for different applications are collected in a library and can be generated by small applications ('apps').
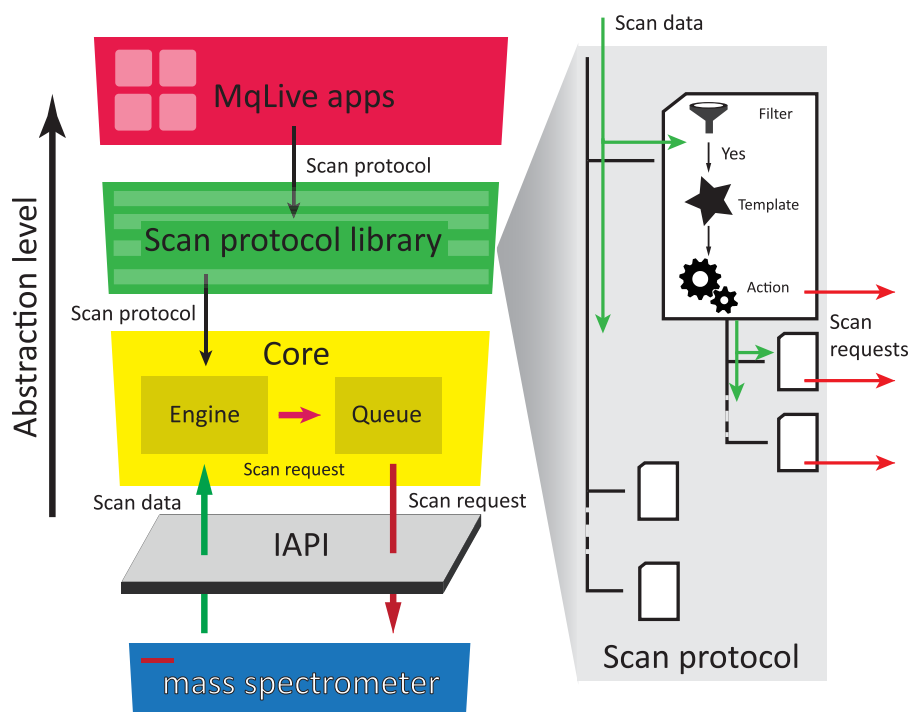
ployed internal standards and are therefore classified as "Tier 3" according to the MCP guidelines. Target peptides were selected randomly as detailed above without considering modification states or uniqueness to proteoforms.

RESULTS

Here we describe the development of a software framework termed MaxQuant.Live for real-time monitoring of mass spectrometric data and controlling of the data acquisition. We demonstrate its usability and performance in terms of scanning speed using a reimplemented topN method. We demonstrate that thousands of peptides of interest can be detected and immediately selected for deeper analysis, greatly extending the toolbox for targeted proteomics. To explore the current limits of our technology, we targeted over 25,000 peptides in a single experiment.

Design and Functionality of MaxQuant.Live—A few years ago, Thermo Fisher Scientific developed an IAPI that enables fast, bidirectional communication between a Q-Exactive mass spectrometer and an outside. We developed a software module, written in the C# programming language, containing functionality for advanced data acquisition and analysis in real-time, which communicates with the mass spectrometer through the IAPI (Experimental Procedures). We termed the program MaxQuant.Live because it forms a bridge between intelligent data acquisition and downstream analysis in the MaxQuant environment. In one direction, the IAPI transmits every measured mass spectrum to our software on the fly and in the other direction it enables MaxQuant.Live to send scan commands to the instrument every time it is ready to

accept new instructions. Fig. 1 illustrates the interplay between the core module of MaxQuant.Live and the mass spectrometer enabled by the IAPI. The engine in Max-Quant.Live executes a run-specific scan protocol (see below) which contains the acquisition strategy for the current LC-MS run and which is loaded from the scan protocol library. The scan requests generated by the engine are stored in the local scan queue before they are pushed sequentially to the MS instrument.

In case the scan queue is empty it periodically sends fallback scan requests to prevent the instrument from running idle or changing its operation status. This design of the scan queue ensures that the core module of MaxQuant.Live keeps control of the instrument during the entire run once a scan protocol has been loaded from the library and while the instrument is connected to the IAPI. Because of this generic additional abstraction layer, our core module is independent of the attached IAPI and could also be combined with instrument control libraries of other mass spectrometers.

The scan protocol specifies the acquisition concept for an LC-MS run. It implements an abstract logic (right panel in Fig. 1) which makes use of a decision tree, a common construct in computer science that has previously been applied in proteomics to select optimal fragmentation modes by Coon and co-workers (39). The decision tree simplifies the development of new acquisition strategies and generates a cascade of scan requests on the basis of the incoming scan containing the

mass spectrum and the associated metadata. Every node of the scan protocol tree consists of three components: A filter, a scan template and data-dependent actions. The filter checks if meta- and spectral data of the incoming scan match particular features. If the check is negative, processing of this node and its children is stopped and the scan protocol tree proceeds to the next item. If the check is positive, for instance because the incoming scan is of type MS1 or contains specific ions of interest, then a new tailored scan request is created based on properties defined in the scan template. This comprises settings for the quadrupole, the collision cell and the mass analyzer. The third component, the data-dependent action, then establishes the connection between the incoming scan data and the settings of the next scan request. Based on its stored data and the incoming data, it chooses particular actions, such as selecting a particular precursor for isolation in the quadrupole, followed by acquisition of a fragmentation spectrum at a particular energy. Only the values that are different from the default template are overwritten. In the simple example of a topN method, the data-dependent action would be restricted to setting the position of the isolation window. After the incoming scan has successfully run through a scan protocol node, it is passed to its children, which may implement additional logic by themselves and trigger further scan requests.

Although scan protocols allow an easy and flexible way to develop acquisition strategies on a high abstraction level, using them is complex and difficult for a nonspecialized mass spectrometry laboratory. For this reason, MaxQuant.Live includes a series of small programs (apps) that can automatically generate scan protocols based on predefined acquisition strategies. We have created an app store for MaxQuant.Live that allows easy access to a collection of apps for different data acquisition strategies, which we have developed and tested in our group. In addition to the strategies described in this publication, BoxCar (40) acquisitions and support for the EASI-tag method (41) are already included.

Usability and Performance of the Software Package—Our ambition was to make MaxQuant.Live very robust and fast, so that any mass spectrometry laboratory can use it for their workflows, without affecting ease of use or throughput. We further aimed to make it universally available and supportable in the long term, like the other parts of the MaxQuant ecosystem.

The graphical user interface (GUI) of MaxQuant.Live unifies the control over all our software components in a user-friendly way, starting from the instrument connection to the scan protocol library and the apps for creation of new acquisition schemes (Fig. 2A). The user can start a scan protocol from the library which then triggers MaxQuant.Live to take control of the mass spectrometer until the end of the run where it switches back to idle mode. It does not interfere with the vendor's software and it can be continuously active in "listen-

ing mode." In this way, acquisition can seamlessly switch between Xcalibur and MaxQuant.Live.

The user initially selects the app from the built-in app store for the desired workflow. MaxQuant.Live allows the creation of new scan protocols without knowledge of the underlying decision tree structure using simple GUIs that break down the complexity of each scan protocol into a small number of required settings. Fig. 2A illustrates this for the GUI of the topN app, which reimplements the standard data-dependent acquisition scheme as a benchmark example. After the user specifies the parameters, the app generates the corresponding scan protocol and adds it to the scan protocol library. The GUI also allows editing a scan protocol within the app at later time points to modify the acquisition strategy.

In our topN implementation, the peak selection can be restricted to specific charge states and intensity values/ranges to focus fragmentation on preferred classes. As in Xcalibur, resequencing of precursors can be prevented. Additionally, the relevant instrument parameters for the MS1 survey as well as the MS2 fragmentation scans can be specified in the GUI.

To benchmark the acquisition speed of a mass spectrometer under the control of MaxQuant.Live, we performed standard HeLa LC-MS/MS runs using our implementation of the top15 method. MaxQuant.Live achieved at least as many MS2 scans per second over the full 120 min gradient as the vendor's software (Fig. 2B). (The faster speed at the beginning of the gradient is likely because the Xcalibur peak selection algorithm uses a different intensity threshold.) This indicates that both MaxQuant.Live and the IAPI are extremely fast, and do not impose any relevant overhead in acquisition compared with direct control by Xcalibur. In particular, the total number of MS2 scans and peptide spectrum matches (PSMs) is not compromised, creating a solid basis for more intelligent acquisition schemes.

Three-dimensional Adaptive Control for Peptide Recognition in Real-time—Having established a fast and robust framework for data-dependent acquisition, we next set out to accurately recognize eluting peptides in real-time at a very large scale. This is challenging because hundreds of precursor ions elute at any given time in complex proteome analysis and the elution time for every peptide subtly shifts from run to run. As a result, existing "inclusion lists" and "exclusion lists" are in practice limited to a relatively small number of precursors. In contrast, the ability to detect large numbers of peptides should enable MaxQuant.Live to take data-dependent decisions about the next scan operations in real-time and thereby to realize more intelligent acquisition strategies.

MaxQuant.Live includes a powerful app that implements diverse strategies to target specific precursor ions in an LC-MS run. They build on a real-time feature detection algorithm combined with adaptive nonlinear corrections in the retention time, *m/z* and intensity dimensions.
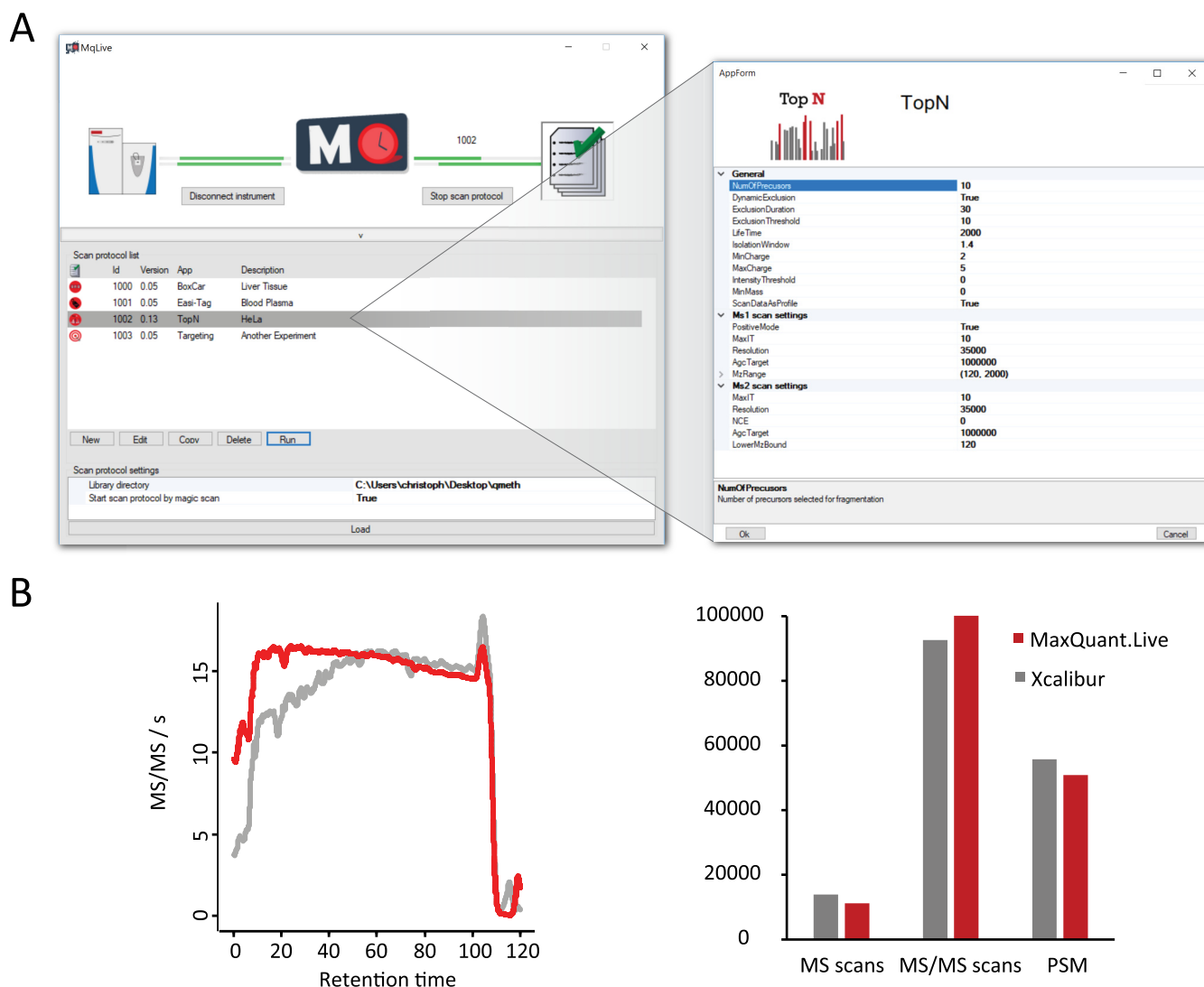
A

B

FIG. 2. **Ease of use and acquisition speed of MaxQuant.Live.** *A*, Graphical user interface containing functionalities to create and manage scan protocols. *B*, Benchmarking the acquisition speeds of MaxQuant.Live *versus* the vendor's software (Xcalibur). In both top15 implementations, the instrument was acquiring MS2 spectra at nearly the maximum rate throughout the run (left panel). The number of MS and MS2 scans as well as the peptide spectrum matches (PSM) are comparable (right panel).

In the list of centroid *m/z* values received from the instrument, our software determines isotope patterns, which are then compared with a list of precursor ions of know mass, charge state, intensity and estimated retention time. For a potential match, the ion intensity must first exceed a threshold, which is a user-defined percentage of the expected intensity. This is calculated from the first two isotopic peaks, which are assumed to conform to the averagine-model (42), as is the case in MaxQuant post-processing, and which must have the expected mass-to-charge difference within a user-defined tolerance of several ppm. MaxQuant.Live sets the recorded ion intensity to zero if either of the two peaks are missing or if there is an interfering peak before the presumed monoisotopic peak.

The second condition of the recognition algorithm requires that the precursor elutes within a certain time window around its expected retention time. Depending on a variety of external factors, peptide elution times can shift by several minutes between any two LC-MS runs, with the consequence that "retention time windows" are generally set to several minutes. For very large numbers of targeted precursors, this would lead to too many potential matches to eluting features. To tackle this problem, we extended the recognition algorithm by an adaptive nonlinear correction of the observed retention time shifts that is inspired by the "match between runs" approach of MaxQuant (27). Briefly, we use a subset of easily recognizable peptides to continuously minimize the median differences between the observed and the expected retention times. Because of applying dynamic corrections we can dramatically shrink the tolerances for the elution time values that are used in the ion recognition. In a typical run, the interval containing 95% of the expected precursors shrinks from sev-
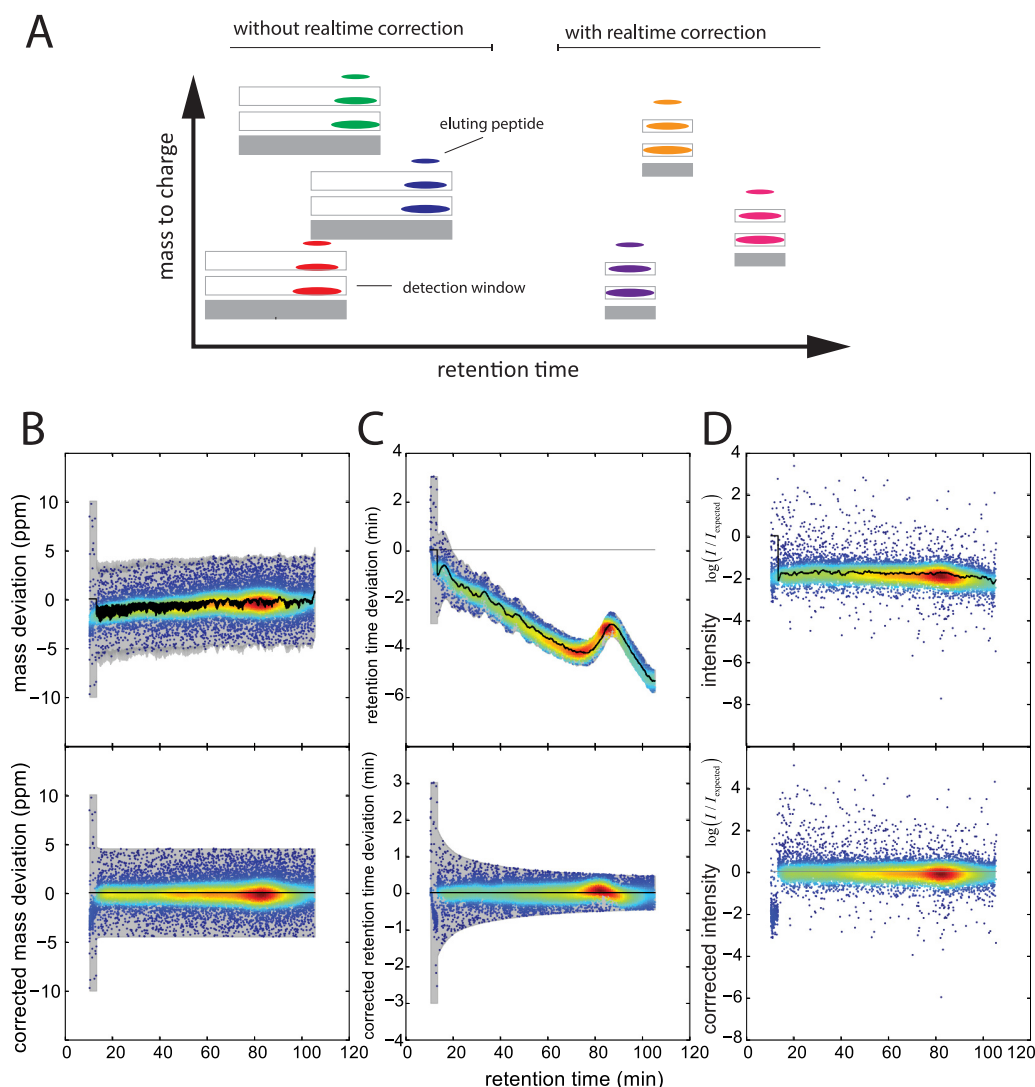
FIG. 3. **MaxQuant.Live targeting application.** *A*, Real-time peptide recognition expects the first two isotopic peaks within a dynamic retention time and mass-to-charge tolerance window as indicated by the gray boxes. Our adaptive correction approach continuously corrects observed global shifts of the elution time, mass calibration and peptide intensity and reduces the tolerances to minimum values. *B–D*, application of the dynamic global corrections (black lines) during an LC-MS run (upper row) drastically narrows the recognition algorithm tolerances (gray areas in *B* and *C*) and the scaling of the peptide intensities to the values observed in the reference run.

eral minutes to less than 1 min (Fig. 3*A*). Although similar "dynamic corrections" have been applied by us and others before, MaxQuant.Live achieves high robustness and precision by using a very large number of peptide precursors for real time correction (up to thousands).

Like the retention time alignment, mass accuracy can be greatly improved with the help of subsets of peptides that serve as internal calibrants (43). Based on the same principle as above, we therefore continuously recalibrate the mass scale, achieving severalfold improvements in real time mass accuracy. However, in contrast to MaxQuant, our mass correction applies to each entire spectrum, rather than being peptide specific. For the example in Fig. 3*B*, the a priori mass window could be reduced from a maximum mass deviation

±10 ppm to ±4.5 ppm which is the same maximum value as used in MaxQuant post-processing.

Signal intensity is the third dimension of precursor features and its adaptive control accounts for day to day differences in sensitivity of the LC-MS set up. Given the signals of the reference peptide population, an overall scaling factor is applied to make the recorded signal intensities comparable to the ones in the targeting list generated from a reference run. In our experiments we noticed that this scaling factor varied between different runs, for example as a result of varying sample amounts on column, but only little within a single run (Fig. 3*C*).

Targeted Acquisition of Breakdown Curves—Robust and precise peptide recognition in real-time should open various
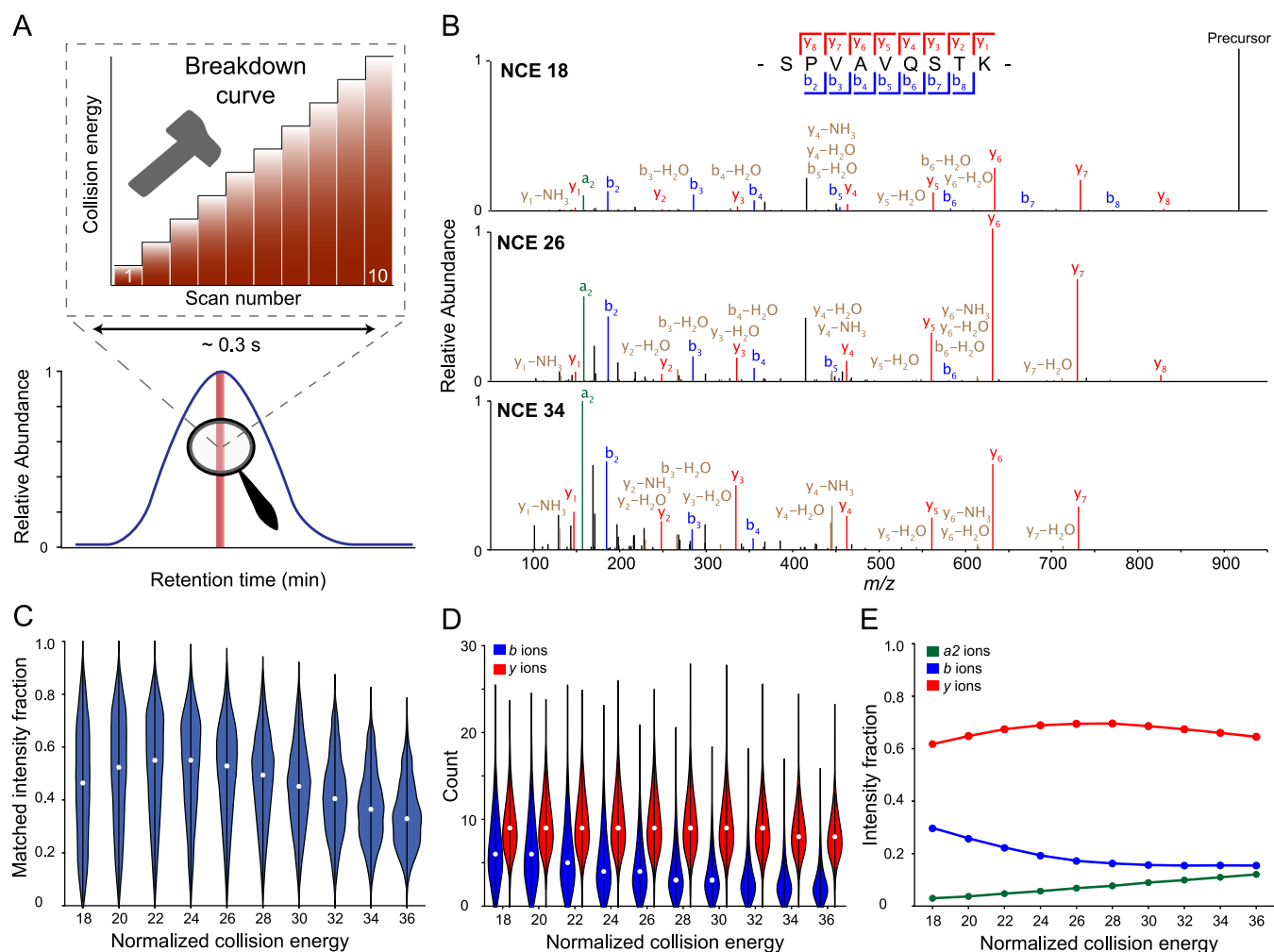
FIG. 4. **Automated acquisition of peptide breakdown curves.** *A*, Extracted ion chromatogram of a targeted peptide. On detection, MaxQuant.Live acquires repeated MS2 scans of this precursor with increasing collision energies. *B*, Exemplary spectra from a single breakdown curve. *C*, Fraction of the total MS2 ion current annotated by the Andromeda search engine as a function of the normalized collision energy. *D*, Number of identified b and y ions as a function of the normalized collision energy. *E*, Median summed intensity of a2, b, and y ions relative to the sum of all identified fragment ions. $n = 962$ peptides.

opportunities for advanced analysis of selected peptides. To demonstrate this, we chose to generate "breakdown curves," which are useful to determine optimal collision energies of peptides or to determine the structure of metabolites. We directed MaxQuant.Live to detect a subset of 1000 peptides in a complex HeLa background and fragment each of them with increasing collision energies. Using 10,000 abundant background peptides for our adaptive real-time correction, the monitoring time for each of the peptides of interest was reduced to less than 4 min in the 120 min runs. Notably, the median absolute retention time deviation was only 0.2 min after recalibration in all three replicates (supplemental Fig. S1). Together with the sub-ppm mass accuracy, this allowed us to successfully acquire breakdown curves for 962 of the 1000 targeted peptides. Fig. 4*A* illustrates the method for a specific target peptide (SPVAVQSTK). We used ten different collision energies from NCE 18 to 36 at a mass resolution of 15,000 at

m/z 200, which translates into a net analysis time of only 0.3 s per breakdown curve. Three example spectra for low, middle and high collision energies are annotated in Fig. 4*B*. At NCE 18, the spectrum was dominated by the precursor ion, indicating incomplete fragmentation. Despite the relatively low abundance of fragment ions, we observed the complete y ion series (y_1–y_8) as well as the complementary b_2 to b_8 ion series. At NCE 26, the precursor ion was completely fragmented. Increasing the NCE further yielded low-mass immonium ions and many internal fragment ions, which escaped automatic scoring with the Andromeda search engine (44). The possibility to target thousands of peptides enables global analysis of peptide fragmentation. To illustrate uses of this capability, we plotted the fraction of the fragment ion current that has been identified as a function of the collision energy (Fig. 4*C*). This value peaked at NCE 22–24, presumably because of the less frequent generation of internal fragment ions. Generally, we

noted a wide distribution for the peptide specific optimal NCEs, highlighting sequence-dependent differences in the fragmentation efficiency even with the normalized collision energies. Next, we investigated the energy-dependent generation of b and y ions (Fig. 4*D*). B ions were preferably generated at lower collision energies, whereas the number of annotated y ions increased with higher collision energy. Over 60% of the annotated ion current was accounted for by y ions throughout all NCEs, while the relative abundance of b ions was decreasing (Fig. 4*E*). Interestingly, the fraction of the a2 fragment ion in the characteristic a2 -b2 ion pair that is formed instead of the b1 ion, increased up to 15% of the annotated fragment ion current at higher collision energies.

Predictive Multiplexed Selective Ion Monitoring (pmSIM)— In the example above, the MS1 signal of a targeted peptide triggered the acquisition of MS2 scans. However, MS1 spectra can be incomplete in that low abundance precursors may be present in some but not other runs. Thus, instead of relying on the MS1 trigger signal and motivated by the high accuracy of the real-time retention time alignment described above, we next predicted the elution of target peptides based on the endogenous background population (Fig. 5*A*).

To demonstrate our approach, we set up a SILAC (30) experiment in which heavy and light whole-cell HeLa digests were mixed in a 1:4 ratio. In DDA, the limited dynamic range of the full scan resulted in many missing heavy-to-light ratios in the low intensity range (Fig. 5*B*) and overall, MaxQuant reported ratios for only ~60% of the identified peptides. The sensitivity can be boosted dramatically by isolating and selectively accumulating narrow *m/z* ranges, which results in improved MS1 (SIM) or, when fragmented, MS2 quantification (termed parallel reaction monitoring "PRM," when used in targeting studies (15)). Without adaptive retention time alignment, such scans must be repeated over a time range large enough to account for the typical shifts and fluctuations in the elution times. This typically results in a very large overhead of scans for each targeted peptide, limiting the total number that can be studied in a single LC-MS run. Here, we used a "predictive multiplexed SIM" (pmSIM) method to measure heavy and light SILAC peptides simultaneously.

We selected 5000 high abundant peptides as correction peptides for the adaptive real-time corrections (Fig. 5*A*). The correction algorithm of MaxQuant.Live dynamically centered the observation time ranges around the peptide elution times (Fig. 5*C*, colored lines and circles, respectively), yielded an accurate prediction of the time range in which each peptide was expected to elute. This resulted in two times smaller window sizes compared with the initial values. The comparison of the window sizes with the deviations of the peptide apex times from the predictions (Fig. 5*C*, histogram) shows that the time windows could have been chosen smaller. It should be noted that our settings were very conservative and the number of target peptides could be much higher.

To validate the accuracy of our prediction algorithm, we selected 50 peptides from the low abundance range with missing ratios from our SILAC HeLa study (Fig. 5*B*). We then used the MaxQuant.Live targeting app to specify an acquisition method that executed SIM scans of the corresponding ion pairs repeatedly over the expected elution time range. The pmSIM strategy correctly quantified the ratios for the targeted peptides close to the expected value of 4:1 with a median CV of 8.2% (Fig. 5*D*). This is notable, because none of the heavy labeled peptides was quantified at the MS1 level before. The example in Fig. 5*E* shows the increase in sensitivity by comparing the MS1 with the corresponding SIM scan. In the SIM scan, the injection time for the previously unrecorded heavy peptides is 400 times larger than the injection time of the full scan, drastically improving the quantitative accuracy.

Highly Efficient Proteome Quantification—The examples shown so far demonstrate the ability of MaxQuant.Live to perform a specific and sophisticated analysis of a limited number of peptides of interest. The fact that the underlying peptide recognition algorithm can in principle deal with an unlimited number of peptides, makes applications feasible that target a substantial proportion of the total set of precursor ions. We reasoned that this generically boosts the reproducibility of peptide fragmentation events between LC-MS runs compared with the topN method.

We implemented our strategy using the targeting app of MaxQuant.Live and generated sets with different numbers of targeted peptides, which were randomly selected from triplicate MS analysis of tryptic HeLa lysates using a standard top15 method in Xcalibur (Fig. 6*A*). For every set of peptides, we performed triplicate LC-MS runs in which MS2 scans were triggered if one of the peptides was recognized by our algorithm in the MS1 scans. The number of peptides that were fragmented and correctly identified afterward by MaxQuant is shown in Fig. 6*B* for all six sets of peptides. Although nearly every targeted peptide was hit in at least one of the runs (green line), this fraction decreases for those hit in at least two (blue line) and all three runs (red line), respectively. The quantification precision was comparable to standard DDA runs with coefficients of variation between the triplicate measurements ranging from 10.4%–12.5% (supplemental Fig. S2).

These results indicate that our strategy can target very large numbers of peptides even though some stochasticity remains between the acquisitions in the different runs. This is likely because of some peptides not being recognized by our algorithm at the MS1 level. An analysis of the of the initial topN and the targeting raw data files using MaxQuant with the matching between runs feature showed very similar results. Thus, the well-established feature detection of MaxQuant could not find significantly more spectral features at the MS1 level from the targeting list, even given full information after complete analysis. This suggests that these peptides, which were selected from the original topN runs, are not "visible" at all in the MS1 scans of the targeting runs. A comparison
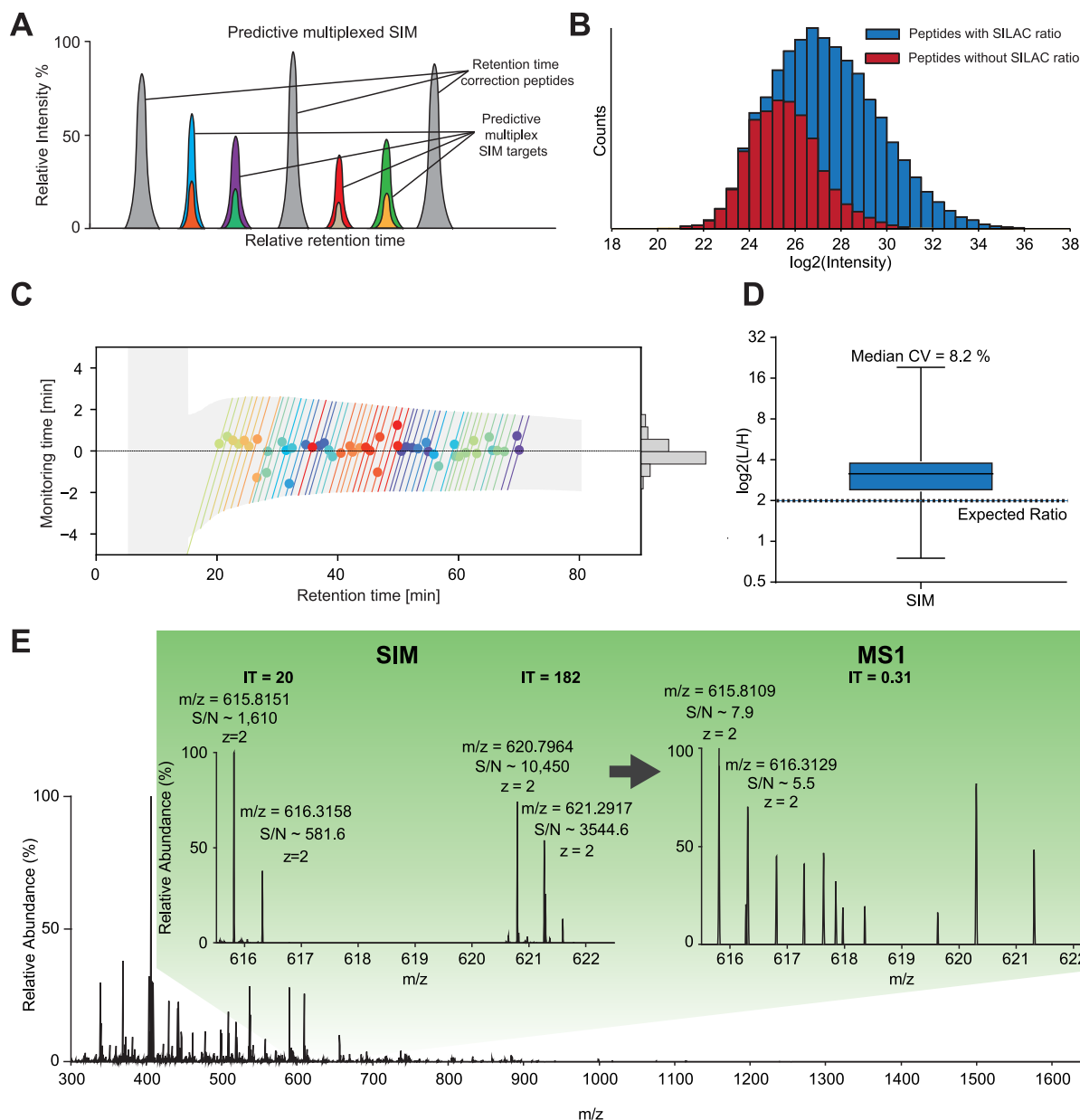
FIG. 5. **Predictive multiplexed SIM (pmSIM).** Peptides employed for live retention time correction are distributed across the gradient and are highly abundant, compared with the low abundant targeted peptides and their SILAC partner needed for quantification (*A*). *B*, Total log2 intensity abundance range of all peptide identifications from the standard run with a light to heavy SILAC ratio of 4:1. In blue, all peptide identifications with identified ratios are highlighted. In red, all peptide identifications in the light channel without any reported SILAC ratios are highlighted. *C*, Watch-time of the predictive multiplexed SIM scan-mode in the targeting experiment. *D*, Resulting SILAC ratios after SIM-targeting using Skyline (35). *E*, Example of a very low abundant target peptide compared in the original MS1 and after pmSIM demonstrating ~40-fold increase of S/N.

of the intensity histograms of the peptides that were successfully targeted and identified by MS/MS in all three runs (Fig. 6*C*, blue) to the ones that were hit in less than three runs (green) shows a slight shift of the intensity distribution to lower values. We therefore suspect that the spectral noise thresholding employed by Xcalibur set the corresponding signals to zero even though they only slightly dipped below acceptance criteria, something we have also

noticed when boosting the dynamic range in the BoxCar acquisition scheme (40). A possible solution to tackle this problem of the acquisition side would be to boost the peptide intensities by using BoxCar scans for the peptide recognition instead of the MS1 scans.

To counter the effect of peptide features missing because of thresholding in our analysis and make the data between the two triplicate measurements comparable, we further normal-
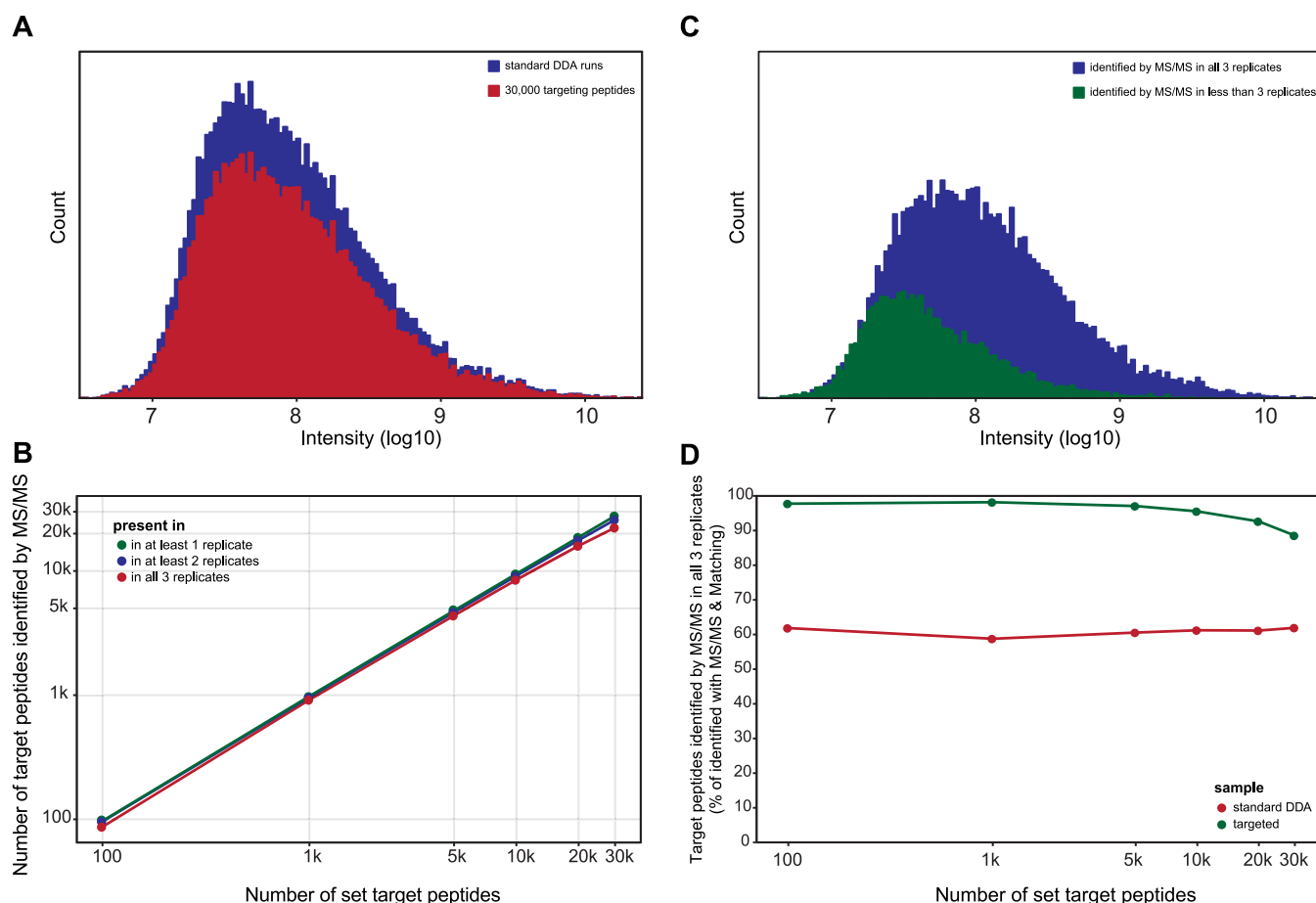
FIG. 6. **Reproducible identification of over 20,000 peptides of interest.** Tryptic HeLa lysates were analyzed by either a standard DDA method designed in the Xcalibur method editor or by the MaxQuant.Live targeting method with 100, 1000, 5000, 10,000, 20,000 or 30,000 targeted peptides. Triplicate injections were performed and sequenced peptides were identified by MaxQuant with or without the matching between runs function activated. *A*, Selected targets were uniformly distributed over the whole intensity range of peptides identified in previous triplicate standard DDA runs. *B*, The number of targets correctly identified by MS/MS. *C*, Intensity distribution of the correctly identified sequences in MaxQuant.Live runs with 30,000 targets. *D*, Percentage of correctly identified targets by MS/MS for the MaxQuant.Live method compared with the identifications by MS/MS in the standard topN method and matching between runs in all three triplicate injections.

ized the number of peptides that were successfully targeted in all triplicate measurements to the number of targeted peptides identified by the matching between runs feature (Fig. 6*D*). The standard top15 method reached about 61% success rate, regardless of the number of peptide precursors. In contrast, in our targeting runs, the normalized percentage of successfully targeted peptides (green line) was 95% and only slightly lower for >20,000 targeted peptides. This effect is presumably related to the fact that the number of co-eluting peptides increases beyond what can be fragmented sequentially by the mass spectrometer in the time available. Although this is not a conceptual limitation of our large-scale targeting approach, it is an opportunity to be addressed by instrument improvements.

DISCUSSION AND CONCLUSION

In bottom-up proteomics, data dependent acquisition and targeted approaches have co-existed for many years. DDA

has been and remains the method of choice for initial characterization of proteomes under study. Conversely, there are many applications, where only a restricted number of peptides is of interest, but these need to be measured consistently over many samples. Although both approaches have become more powerful with the general advances in instrumentation and proteomics technologies, DDA is still not powerful enough to subsume targeted analyses. Conversely, targeted methods have been difficult to establish in a robust manner, enough for clinical use, for instance, especially when monitoring more than a few dozens of peptides.

Here, we made use of the recently developed fast and robust IAPI of the Thermo instruments to interface with the acquisition process in real time. MaxQuant.Live makes use of experimental information as they are acquired to direct the acquisition in a more intelligent way. We have implemented different mass spectrometric acquisition schemes in the form

of small built-in apps. We demonstrated that this workflow is highly performant as it can easily replicate the standard topN methods, for instance, without loss of quality. In targeted schemes, MaxQuant.Live continuously recalibrates the signal coming from the mass spectrometer in retention time, mass and intensity dimensions, allowing a much better prediction of the identity of eluting peptide features than possible previously. This allows, for instance, selecting any subgroup of hundreds of peptides to be targeted for accurate quantification (exemplified by our predictive multiplexed SIM method). In-depth analysis of the fragmentation patterns of large numbers of individual peptides is another valuable addition to the proteomics toolbox, which can be used to optimize precursor-fragment transitions for PRM or to pinpoint and localize modifications of low-abundance proteins. MaxQuant.Live ensures that all peptides are reliably acquired at all collision energies (as opposed to stochastic precursor selection with DDA) and in single runs. In our own group, we have already applied such a strategy to characterize the fragmentation of a novel isobaric tag (41). Even if these methods take much longer than standard fragmentation for the selected peptides, they still do not substantially contribute to overall measuring time. This means that sophisticated measurements could be done on peptides of interest, while still recording the overall proteome. Although we randomly chose peptides, one could, for instance, select a specific class of post-translation modifications, peptides that distinguish between isoforms or any other highly informative class of interest. The resulting, "enhanced," data sets could also become valuable sources for imminent machine-learning approaches (20, 28).

Building on the precise recalibration in MaxQuant.Live, we demonstrate that the scale of such experiments can be readily extended to over 25,000 peptides of interest with very high reproducibility. Conceptually, MaxQuant.Live bridges the approaches of classical shotgun and targeted proteomics. On one hand, when high numbers of peptides are targeted, it resembles shotgun experiments and could be interpreted as a very thorough and much more efficient implementation of inclusion lists (45). On the other hand, when smaller target numbers are addressed, the acquisition strategy resembles classical targeting, however, with more flexibility and much greater robustness because of real-time recalibration. To express the conceptual nature of our approach we call it "global targeting," as it combines desirable aspects of classical shotgun and targeted proteomics.

To analyze such data we therefore resorted to existing tools from both approaches. In the pmSIM experiments, we manually inspected mass spectra and elution profiles of the few target peptides. When we extend this approach to hundreds or thousands of targets, we recommend using established tools for statistically sound identification of targeted peptides such as target-decoy strategies (46). Finally, in experiments with high target peptide numbers we followed a "spectrum centric approach" (47) for precursor identification, like regular shotgun proteomics experiments.

In our global targeting experiments, we observed coefficients of variation that lie in the expected range for classical shotgun experiments at very high numbers of targeted precursors and very close to classical targeting experiments, when these numbers are somewhat reduced. This means that our method unifies the two approaches not only in terms of identifications, but also allows to implicitly define the desired accuracy (within instrument capabilities) via the number of targets beforehand. The same applies to sensitivity, which is limited by the instrument's capabilities and the measurement time per peptide. Global targeting allows the operator to optimally balance target numbers and sensitivity.

We have made MaxQuant.Live freely available and hope that it will stimulate the community into exploring this exciting direction.

DATA AVAILABILITY

The mass spectrometry proteomics data have been deposited to the ProteomeXchange Consortium via the PRIDE (38) partner repository with the dataset identifier PXD011225.

Author contributions: C.W., F.M., and M.M. designed research; C.W., F.M., S.V.W., and A.-D.B. performed research; C.W., F.M., S.V.W., A.-D.B., and M.M. analyzed data; C.W., F.M., S.V.W., A.-D.B., and M.M. wrote the paper; J.C. contributed new reagents/analytic tools; J.C. supervised Dr. Christoph Wichmann.

REFERENCES

1. Lössl, P., van de Waterbeemd, M., and Heck, A. J. (2016) The diverse and expanding role of mass spectrometry in structural and molecular biology. *EMBO J.* **35,** 2634–2657
2. Larance, M., and Lamond, A. I. (2015) Multidimensional proteomics for cell biology. *Nat. Rev. Mol. Cell Biol.* **16,** 269–280
3. Aebersold, R., and Mann, M. (2016) Mass-spectrometric exploration of proteome structure and function. *Nature* **537,** 347–355
4. de Godoy, L. M., Olsen, JV, Cox, J, Nielsen, ML, Hubner, NC, Fröhlich, F, Walther, TC, and Mann, M. (2008) Comprehensive mass-spectrometry-based proteome quantification of haploid versus diploid yeast. *Nature* **455,** 1251–1254
5. Hebert, A. S., Richards, A. L., Bailey, D. J., Ulbrich, A., Coughlin, E. E., Westphall, M. S., and Coon, J. J. (2014) The one hour yeast proteome. *Mol. Cell. Proteomics* **13,** 339–347
6. Bekker-Jensen, D. B., Kelstrup, C. D., Batth, T. S., Larsen, S. C., Haldrup, C., Bramsen, J. B., Sørensen, K. D., Høyer, S., Ørntoft, T. F., Andersen, C. L., Nielsen, M. L., and Olsen, J. V. (2017) An optimized shotgun

strategy for the rapid generation of comprehensive human proteomes. *Cell Syst.* **4,** 587–599.e4

7. Altelaar, A. M., and Heck, A. J. (2012) Trends in ultrasensitive proteomics. *Curr. Opin. Chem. Biol.* **16,** 206–213

8. Röst, H. L., Malmström, L., and Aebersold, R. (2015) Reproducible quantitative proteotype data matrices for systems biology. *Mol. Biol. Cell* **26,** 3926–3931

9. Geyer, P. E., Holdt, L. M., Teupser, D., and Mann, M. (2017) Revisiting biomarker discovery by plasma proteomics. *Mol. Syst. Biol.* **13,** 942

10. Michalski, A., Cox, J., and Mann, M. (2011) More than 100,000 detectable peptide species elute in single shotgun proteomics runs but the majority is inaccessible to data-dependent LC-MS/MS. *J. Proteome Res.* **10,** 1785–1793

11. Ludwig, C., Gillet, L., Rosenberger, G., Amon, S., Collins, B. C., and Aebersold, R. (2018) Data-independent acquisition-based SWATH-MS for quantitative proteomics: a tutorial. *Mol Syst Biol.* **14,** e8126

12. Picotti, P., and Aebersold, R. (2012) Selected reaction monitoring-based proteomics: workflows, potential, pitfalls and future directions. *Nat. Methods* **9,** 555–566

13. Kondrat, R. W., McClusky, G. A., and Cooks, R. G. (1978) Multiple reaction monitoring in mass spectrometry/mass spectrometry for direct analysis of complex mixtures. *Anal. Chem.* **50,** 2017–2021

14. Yost, R. A., and Enke, C. G. (1978) Selected ion fragmentation with a tandem quadrupole mass spectrometer. *J. Am. Chem. Soc.* **100,** 2274–2275

15. Peterson, A. C., Russell, J. D., Bailey, D. J., Westphall, M. S., and Coon, J. J. (2012) Parallel reaction monitoring for high resolution and high mass accuracy quantitative, targeted proteomics. *Mol. Cell. Proteomics* **11,** 1475–1488

16. Bourmaud, A., Gallien, S., and Domon, B. (2016) Parallel reaction monitoring using quadrupole-Orbitrap mass spectrometer: Principle and applications. *Proteomics* **16,** 2146–2159

17. Picotti, P., Rinner, O., Stallmach, R., Dautel, F., Farrah, T., Domon, B., Wenschuh, H., and Aebersold, R. (2010) High-throughput generation of selected reaction-monitoring assays for proteins and proteomes. *Nat. Methods* **7,** 43–46

18. Zauber, H., Kirchner, M., and Selbach, M. (2018) Picky: a simple online PRM and SRM method designer for targeted proteomics. *Nat. Methods* **15,** 156–157

19. Deutsch, E. W., Lam, H., and Aebersold, R. (2008) PeptideAtlas: a resource for target selection for emerging targeted proteomics workflows. *EMBO Rep.* **9,** 429–434

20. Zolg, D.P., Wilhelm, M., Schnatbaum, K., Zerweck, J., Knaute, T., Delanghe, B., Bailey, D. J., Gessulat, S., Ehrlich, H. C., Weininger, M., Yu, P., Schlegl, J., Kramer, K., Schmidt, T., Kusebauch, U., Deutsch, E. W., Aebersold, R., Moritz, R.L., Wenschuh, H., Moehring, T., Aiche, S., Huhmer, A., Reimer, U., vKuster, B. (2017) Building ProteomeTools based on a complete synthetic human proteome. *Nat Methods* **14,** 259–262

21. Kusebauch, U., Campbell, D. S., Deutsch, E. W., Chu, C. S., Spicer, D. A., Brusniak, M. Y., Slagel, J., Sun, Z., Stevens, J., Grimes, B., Shteynberg, D., Hoopmann, M. R., Blattmann, P., Ratushny, A. V., Rinner, O., Picotti, P., Carapito, C., Huang, C. Y., Kapousouz, M., Lam, H., Tran, T., Demir, E., Aitchison, J. D., Sander, C., Hood, L., Aebersold, R., and Moritz, R. L. (2016) Human SRMAtlas: A resource of targeted assays to quantify the complete human proteome. *Cell* **166,** 766–778

22. Gallien, S., Kim, S. Y., and Domon, B. (2015) Large-Scale Targeted Proteomics Using Internal Standard Triggered-Parallel Reaction Monitoring (IS-PRM). *Mol. Cell. Proteomics* **14,** 1630–1644

23. Bailey, D. J., McDevitt, M. T., Westphall, M. S., Pagliarini, D. J., and Coon, J. J. (2014) Intelligent Data Acquisition Blends Targeted and Discovery Methods. *J. Proteome Res.* **13,** 2152–2161

24. Cox, J., and Mann, M. (2008) MaxQuant enables high peptide identification rates, individualized p.p.b.-range mass accuracies and proteome-wide protein quantification. *Nat. Biotechnol.* **26,** 1367–1372

25. Cox, J., Neuhauser, N., Michalski, A., Scheltema, R. A., Olsen, J. V., and Mann, M. (2011) Andromeda: A peptide search engine integrated into the MaxQuant environment. *Proteome Res J* **10,** 1794–1805

26. Graumann, J., Scheltema Ra Zhang, Y., Cox, J., and Mann, M. (2012) A framework for intelligent data acquisition and real-time database searching for shotgun proteomics. *Mol. Cell. Proteomics* **11,** M111.013185

27. Geiger, T., Wehner, A., Schaab, C., Cox, J., and Mann, M. (2012) Comparative proteomic analysis of eleven common cell lines reveals ubiquitous but varying expression of most proteins. *Mol. Cell. Proteomics* **11,** M111.014050

28. Sinitcyn, P., Rudolph, J. D., and Cox, J. (2018) Computational methods for understanding mass spectrometry-based shotgun proteomics data. *Annu. Rev. Biomed. Data Sci.* **1,** 207–234

29. Kuehn A *et al.* (2013) Customized real-time control of benchtop orbitrap MS *in Proceedings of the 61st ASMS Conference on Mass Spectrometry and Allied Topics* Poster MP377

30. Ong, S. E., Blagoev, B., Kratchmarova, I., Kristensen, D. B., Steen, H., Pandey, A., and Mann, M. (2002) Stable isotope labeling by amino acids in cell culture, SILAC, as a simple and accurate approach to expression proteomics. *Mol Cell Proteomics* **1,** 376–386

31. Ong, S. E., and Mann, M. (2006) A practical recipe for stable isotope labeling by amino acids in cell culture (SILAC). *Nat. Protoc.* **1,** 2650–2660

32. Kulak, N. A., Pichler, G., Paron, I., Nagaraj, N., and Mann, M. (2014) Minimal, encapsulated proteomic-sample processing applied to copy-number estimation in eukaryotic cells. *Nat. Methods* **11,** 319–324

33. Kelstrup, C. D., Bekker-Jensen, D. B., Arrey, T. N., Hogrebe, A., Harder, A., and Olsen, J. V. (2018) Performance evaluation of the QExactive, H. F.-X for shotgun proteomics. *Proteome Res. J.* **17,** 727–738

34. Olsen, J.V., Macek, B., Lange, O., Makarov, A., Horning, S., and Mann, M. (2007) Higher-energy C-trap dissociation for peptide modification analysis. *Nat. Methods* **4,** 709–712

35. MacLean, B., Tomazela, D. M., Shulman, N., Chambers, M., Finney, G. L., Frewen, B., Kern, R., Tabb, D. L., Liebler, D. C., and MacCoss, M. J. (2010) Skyline: an open source document editor for creating and analyzing targeted proteomics experiments. *Bioinformatics* **26,** 966–968

36. Tyanova, S., Temu, T., Sinitcyn, P., Carlson, A., Hein, M. Y., Geiger, T., Mann, M., and Cox, J. (2016) The Perseus computational platform for comprehensive analysis of (prote)omics data. *Nat. Methods* **13,** 731–740

37. R Core Team (2008) R: A language and environment for statistical computing. *R Foundation for Statistical Computing, Vienna, Austria*. ISBN 3-900051-07-0, URL http://www.R-project.org

38. Vizcaíno, J. A., Csordas, A., Del-Toro, N., Dianes, J. A., Griss, J., Lavidas, I., Mayer, G., Perez-Riverol, Y., Reisinger, F., Ternent, T., Xu, Q. W., Wang, R., and Hermjakob, H. (2016) 2016 update of the PRIDE database and its related tools. *Nucleic Acids Res.* **44,** D447–D456

39. Swaney, D. L., Mcalister, G. C., and Coon, J. J. (2008) Decision tree-driven tandem mass spectrometry for shotgun proteomics. *Nat. Methods* **5,** 959–964

40. Meier, F., Geyer, P. E., Virreira Winter, S., Cox, J., and Mann, M. (2018) BoxCar acquisition method enables single-shot proteomics at a depth of 10,000 proteins in 100 minutes. *Nat. Methods* **15,** 440–448

41. Virreira Winter, S., Meier, F., Wichmann, C., Cox, J., Mann, M., and Meissner, F. (2018) EASI-tag enables accurate multiplexed and interference-free MS2-based proteome quantification. *Nat. Methods* **15,** 527–530

42. Senko, M. W., Beu, S. C., and McLafferty, F. W. (1995) Determination of monoisotopic masses and ion populations for large biomolecules from resolved isotopic distributions. *J. Am. Soc. Mass Spectrom.* **6,** 229–233

43. Cox, J., Michalski, A., and Mann, M. (2011) Software lock mass by two-dimensional minimization of peptide mass errors. *J. Am. Soc. Mass Spectrom.* **22,** 1373–1380

44. Neuhauser, N., Michalski, A., Cox, J., and Mann, M. (2012) Expert system for computer-assisted annotation of MS/MS Spectra. *Mol. Cell. Proteomics* **11,** 1500–1509

45. Schmidt, A., Claassen, M., and Aebersold, R. (2009) Directed mass spectrometry: towards hypothesis-driven proteomics. *Curr. Opin. Chem. Biol.* **13,** 510–517

46. Reiter, L., Rinner, O., Picotti, P., Hüttenhain, R., Beck, M., Brusniak, M. Y., Hengartner, M. O., and Aebersold,. R. (2011) mProphet: automated data processing and statistical validation for large-scale SRM experiments. *Nat. Methods* **8,** 430–435

47. Ting, Y. S., Egertson, J. D., Payne, S. H., Kim, S., MacLean, B., Käll, L., Aebersold, R., Smith, R. D., Noble W. S., and MacCoss M. J. (2015) Peptide-centric proteome analysis: an alternative strategy for the analysis of tandem mass spectrometry data. *Mol. Cell. Proteomics* **14,** 2301–2307